Am J Transl Res 2026;18(3):2522-2535
www.ajtr.org /ISSN:1943-8141/AJTR0171285

Original Article

Banxia Xiexin Decoction inhibits chemoresistance in gastric cancer by regulating BMSC-derived exosome-mediated G3BP1-YWHAZ protein interaction

Fan Yang[1,2*], Senyu Liu[3*], Zhongbo Zhu[1], Lijuan Shi[1], Qingmiao Wang[1], Kun Niu[2], Xiping Liu[1]

[1]*Gansu Engineering Laboratory for New Products of Traditional Chinese Medicine, Gansu Key Laboratory of TCM Excavation and Innovative Transformation, Gansu University of Chinese Medicine, Lanzhou 730000, Gansu, China;* [2]*College of Traditional Chinese Medicine, Hainan Medical University, Haikou 571199, Hainan, China;* [3]*The First Affiliated Hospital of Hainan Medical University, Haikou 571199, Hainan, China.* [*]*Equal contributors.*

Received January 6, 2026; Accepted February 13, 2026; Epub March 15, 2026; Published March 30, 2026

Abstract: Objective: To investigate whether Banxia Xiexin Decoction (BXD) reverses bone marrow mesenchymal stem cell (BMSC)-derived exosome-induced oxaliplatin resistance in gastric cancer (GC) and to elucidate the underlying mechanism. Methods: Oxaliplatin-resistant HGC-27 cells and human BMSCs were cultured in vitro. Exosomes were isolated and characterized by transmission electron microscopy and marker analysis. Cell viability was assessed using CCK-8 assays. Apoptosis, multidrug resistance proteins (MDR, MRP, LRP), stress granule (SG) formation, and G3BP1-YWHAZ interaction were examined by flow cytometry, immunofluorescence, Western blotting, and co-immunoprecipitation. A nude mouse xenograft model was used to evaluate in vivo effects. Results: BMSC-derived exosomes enhanced oxaliplatin resistance in HGC-27 cells, reduced apoptosis, upregulated MDR-related proteins, promoted SG formation, and strengthened G3BP1-YWHAZ interaction. BXD-containing serum reversed these effects by restoring apoptosis, increasing Bax and cleaved caspase expression, suppressing resistance-associated proteins and SG assembly, and disrupting G3BP1-YWHAZ binding. In vivo, BXD attenuated exosome-mediated chemoresistance, inhibited tumor growth, and enhanced oxaliplatin-induced apoptosis. Conclusion: BMSC-derived exosomes promote oxaliplatin resistance in GC through activation of the G3BP1-YWHAZ axis. BXD restores chemosensitivity by interfering with this exosome-mediated pathway, supporting its use as a potential adjuvant strategy to overcome chemotherapy resistance.

Keywords: Banxia Xiexin Decoction, gastric cancer, exosomes, chemoresistance, G3BP1, YWHAZ

Introduction

Gastric cancer ranks third in global incidence and second in cancer-related mortality, remaining a major health burden despite advances in diagnosis and treatment [1, 2]. Systemic chemotherapy continues to be a cornerstone for patients with advanced or metastatic disease. However, the emergence of chemoresistance significantly limits therapeutic efficacy and remains a major obstacle in clinical management [3]. Chemoresistance is a multifactorial and dynamic process involving complex molecular networks that are not yet fully understood [4]. Therefore, elucidating the mechanisms underlying drug resistance and identifying effective strategies to restore chemosensitivity are critical for improving treatment outcomes in gastric cancer.

Increasing evidence highlights the pivotal role of the tumor microenvironment in modulating tumor response to chemotherapy [5]. Mesenchymal stem cells (MSCs), an essential stromal component, actively participate in tumor progression by regulating cancer cell proliferation, invasion, metastasis, and therapeutic response [6, 7]. In gastric cancer, MSC recruitment and functional reprogramming have been linked to tumor development and progression [8-10]. Importantly, MSCs have been identified as key regulators of chemotherapeutic sensitivity, con-

https://doi.org/10.62347/JGWB1234

tributing to the acquisition of drug resistance [11].

Exosomes, small extracellular vesicles released by various cell types, have emerged as critical mediators of intercellular communication within the tumor microenvironment. Chemotherapeutic stress can enhance exosome secretion, and these vesicles have been implicated in transmitting chemoresistance signals among tumor cells [12, 13]. MSC-derived exosomes, in particular, have been shown to promote drug resistance in multiple malignancies, including gastric cancer and multiple myeloma [14]. Experimental studies demonstrate that MSC-derived exosomes confer resistance to agents such as cisplatin and 5-fluorouracil in gastric cancer models both in vitro and in vivo [15]. Mechanistically, these vesicles enhance tumor cell survival by activating anti-apoptotic pathways, thereby reducing chemosensitivity [16, 17].

Apoptosis is the principal mechanism through which most chemotherapeutic agents eliminate tumor cells [18, 19]. Dysregulation of apoptotic signaling, including altered expression of pro- and anti-apoptotic proteins, plays a central role in chemoresistance [20]. Although MSC-derived exosomes have been associated with resistance, the precise mechanisms by which they enhance anti-apoptotic capacity in gastric cancer remain incompletely defined [21]. Recent studies indicate that G3BP1, a core component of stress granules, interacts with YWHAZ to suppress the pro-apoptotic protein Bax, thereby promoting cell survival under stress conditions [22, 23]. This G3BP1-YWHAZ axis represents a potential molecular link between stress responses and chemotherapy resistance.

From the perspective of traditional Chinese medicine (TCM), gastric cancer corresponds to disease categories such as “yege”, “fuliang”, and “zhengji” [24]. Its pathogenesis is traditionally attributed to deficiency of vital qi, accumulation of phlegm, and persistence of pathogenic toxins. The concept of “cancer toxin”, described as unresolved pathogenic factors resulting from imbalance of qi, blood, and organ function, has been proposed to underlie tumor development and progression [25, 26].

Banxia Xiexin Decoction, a classical TCM formula, has demonstrated antitumor activity in gastric cancer through modulation of inflammatory signaling and immune-related pathways [27, 28]. In parallel, accumulating evidence suggests that MSC-derived exosomes can reprogram gastric cancer cells, enhancing proliferation, invasion, and drug resistance [29, 30]. Clinically, modified Banxia Xiexin Decoction has shown potential in improving chemotherapy response.

Based on these observations, the present study employed in vitro and in vivo models of gastric cancer chemoresistance to investigate whether Banxia Xiexin Decoction can restore oxaliplatin sensitivity by targeting MSC-derived exosome-mediated signaling. Specifically, we explored the role of the G3BP1-YWHAZ axis in exosome-driven resistance and evaluated the therapeutic potential of Banxia Xiexin Decoction.

Methods

Reagents

RPMI-1640 (A4192301; Gibco, USA), fetal bovine serum (10099-141; Gibco), trypsin (C0201; Beyotime, China), dimethyl sulfoxide (DMSO; D2650; Sigma-Aldrich, USA), and oxaliplatin (MedChemExpress; lot 343662) were used for cell-based assays. Cell viability was measured using CCK-8 (C0039; Beyotime). Apoptosis was assessed using an Annexin V-FITC/PI kit (40302ES60; YEASEN, China). Protein concentration was determined using a BCA kit (T9300A; Takara, Japan). Co-immunoprecipitation employed Protein A/G Plus Agarose (C600689-0020; BBI Life Sciences, China). Histological and apoptosis staining kits included H&E (G1120; Solarbio, China) and TUNEL (C1098; Beyotime).

Primary antibodies were as follows: anti-MDR (sc-55510), anti-MRP (sc-18874), anti-LRP (sc-57351) (all Santa Cruz Biotechnology, USA), anti-G3BP1 (ab181150; Abcam, UK), anti-YWHAZ (ER62525; Huabio, China), anti-Ki67 (HA721115; Huabio), and and anti-β-actin (Huabio). Rabbit IgG (bs-0295P; Biosynthesis Biotechnology, China) served as a control. Secondary antibodies included Cy3-labeled goat anti-rabbit IgG and HRP-conjugated goat anti-rabbit/anti-mouse IgG (Beyotime, China).

Preparation of Banxia Xiexin Decoction

Banxia Xiexin Decoction was prepared using the classical prescription: Pinelliae Rhizoma (Banxia, 15 g), Zingiberis Rhizoma (Ganjiang, 15 g), Scutellariae Radix (Huangqin, 15 g), Ginseng Radix et Rhizoma (Renshen, 15 g), Glycyrrhizae Radix et Rhizoma (Gancao, 10 g), Coptidis Rhizoma (Huanglian, 6 g), and Jujubae Fructus (Dazao, 4 pieces; ~12 g). All herbs were purchased from Tongrentang Pharmacy and authenticated according to the Chinese Pharmacopoeia (2020 edition).

Herbs were mixed, soaked in water for 30 min, and decocted twice. The first extraction used 8× water (w/v) and was boiled for 1 h; the supernatant was collected. The residue was re-decocted using 6× water (w/v) for 30 min, and the two extracts were combined. After centrifugation, filtration, and concentration, the final stock was adjusted to 2.31 g raw herbs/mL, corresponding to the mouse-equivalent dose converted by body surface area (70 kg adult vs. nude mice).

Ethics statement

Adult SPF Sprague-Dawley rats (6-8 weeks, 250-300 g; 10 males and 10 females) were obtained from Henan Sikebeisi Biological Technology Co., Ltd. (SCXK (Yu) 2020-0005; Quality certificate Nos. 410000000000009319 and 410000000000009320). Bone marrow mesenchymal stem cells (BMSCs) were sourced from Chongqing Western Biotechnology Co., Ltd. A total of 22 SPF male BALB/c-nu nude mice (4-5 weeks, 15-17 g) were purchased from Beijing Huafukang Bioscience Co., Ltd. (SCXK (Jing) 2024-0003). Animals were maintained under SPF conditions (23-25°C; 12-h light/dark cycle) with ad libitum access to food and water. All procedures were approved by Hainan Medical University and conducted in accordance with institutional guidelines, with efforts made to minimize animal numbers and distress.

Preparation of BXD-containing serum

Drug-containing serum was generated in two groups: blank serum (Group A) and BXD serum (Group B). Rats were fasted for 12 h, weighed, and gavaged at 7 mL/kg. Group B received Banxia Xiexin Decoction, whereas Group A received the same volume of saline. The decoction was warmed in a 55°C water bath and cooled to room temperature before administration.

Rats received three gavages (first and second doses 1 day apart; second and third doses 3 h apart). Blood was collected 2 h after the third gavage. Animals were anesthetized with 7% chloral hydrate (1.5 mL/kg, i.p.), and blood was obtained by sterile cardiac puncture and centrifuged (3000 rpm, 20 min, 4°C). Serum was heat-inactivated at 56°C for 30 min and stored at -20°C until use.

Cell culture

The oxaliplatin-resistant gastric carcinoma cell line HGC-27/L was purchased from Shanghai Wenyebio Biotechnology Co., Ltd. Cells were maintained in DMEM supplemented with 10% FBS and 1% penicillin/streptomycin at 37°C with 5% CO_2. To preserve the resistant phenotype, 1 μM oxaliplatin was included in routine culture. For experiments not involving oxaliplatin treatment, resistant cells were passaged at least twice in drug-free medium and used during logarithmic growth.

Xenograft model and treatments

Sample size was determined using G*Power (v3.1) based on pilot data (Cohen's $d = 0.8$, $\alpha = 0.05$, power = 0.80), yielding ≥ 6 mice/group; one additional mouse per group was included to account for ~10% attrition (7 mice/group). Mice were randomized by block randomization (block size = 4) using a computer-generated sequence prepared by an investigator not involved in interventions or outcome assessment. Allocation was concealed in numbered, opaque envelopes. Procedures were conducted under blinded conditions using coded group labels until data analysis was completed.

After 1 week acclimatization, tumor xenografts were established by subcutaneous injection of a cell suspension (100 μL/mouse) into the right axilla. Body weight and tumor size were measured every 2 days, and tumor volume was plotted as a growth curve. When tumors reached 50-100 mm^3 (Day 8), mice received daily intraperitoneal oxaliplatin (10 mg/kg). In parallel, Groups B and C received peritumoral injections of exosomes (10 μg in 100 μL, every

3 days). Group C additionally received oral gavage of the full BXD prescription daily for 3 weeks.

At endpoint, mice were weighed and anesthetized, tumors were excised and photographed, and tissues were allocated for: 4% paraformaldehyde (H&E), 2.5% glutaraldehyde (electron microscopy), or snap-freezing at -80°C (Western blot and other assays).

CCK-8 assay

Cells were seeded for 12 h and then treated according to the experimental design with oxaliplatin (various concentrations), hMSC-derived exosomes (20 μg/mL), and/or BXD-containing serum (three replicates/group). After 24 or 48 h, 10 μL CCK-8 was added per well and incubated for 1-4 h. Absorbance was read at 450 nm. Cell viability (%) was calculated as: $[(OD_{treat}-OD_{blank})/(OD_{control}-OD_{blank})] \times 100\%$. The inhibition rate was calculated as 1 - viability.

Flow cytometry

HGC-27/L cells were plated in 6-well plates. At ~50-60% confluence, medium was replaced with fresh medium containing or lacking oxaliplatin (5 μg/mL), hMSC-derived exosomes (20 μg/mL), and/or drug-containing serum, and incubated for 3 h. Cells were collected (including adherent cells after trypsinization), washed, and resuspended in binding buffer.

Approximately 1-5 × 10^5 cells were stained with 5 μL Annexin V-FITC in 185 μL binding buffer for 10 min at room temperature in the dark, followed by 5 μL PI. Samples were kept on ice and analyzed immediately by flow cytometry.

Immunofluorescence

Cells were washed with PBS (3 × 3 min). After blocking, samples were incubated with primary antibodies against G3BP1 (1:500) and YWHAZ (1:200). Primary incubation was performed either overnight at 4°C or for 90 min at room temperature in a humidified chamber. After PBS washes (3 × 3 min), samples were incubated with FITC- or Cy3-conjugated secondary antibodies (1:800) for 1 h in the dark. Nuclei were counterstained with DAPI for 5 min, washed, mounted with anti-fade medium, and imaged using a confocal microscope.

Western blot

Total protein was extracted, quantified, and 20 μg per lane was separated on 10% SDS-PAGE and transferred to PVDF membranes. Membranes were blocked with 5% milk in TBST and incubated overnight at 4°C with primary antibodies against MDR (sc-55510), MRP (sc-18874), LRP (sc-57351), G3BP1 (ab181150), YWHAZ (ER62525), and β-actin (loading control). After TBST washes, membranes were incubated for 1 h at room temperature with species-matched HRP-conjugated secondary antibodies. Signals were developed using ECL, quantified using ImageJ, and normalized to β-actin.

Transmission electron microscopy (TEM)

Exosome suspensions were diluted in PBS, and 10 μL was applied to Formvar-carbon-coated copper grids for 20 min. Grids were washed on PBS droplets, fixed with 2.5% glutaraldehyde (5 min), rinsed with ultrapure water, stained with uranyl oxalate (pH 7.0, 5 min), and embedded in methylcellulose-uranyl acetate on ice (10 min). After blotting excess liquid, grids were air-dried (5-10 min) and examined by TEM at 80 kV.

Co-immunoprecipitation (Co-IP)

Whole-cell lysates from HGC-27/L cells were prepared using a mild, non-denaturing lysis buffer. For each reaction, 500 μg of protein was incubated overnight at 4°C with antibodies against G3BP1 or YWHAZ (reciprocal Co-IP). Immune complexes were captured using Protein A/G agarose beads, with nonspecific IgG as a negative control. After washing and elution, precipitated proteins were analyzed by immunoblotting with the corresponding antibodies.

Histopathology (H&E)

Excised xenograft tumors were fixed in 4% paraformaldehyde, embedded in paraffin, and sectioned at 4 μm. Sections were deparaffinized, rehydrated, stained with hematoxylin and eosin, dehydrated, cleared, and mounted.

Morphological features were assessed by light microscopy.

TUNEL assay

Tumor tissues were fixed, paraffin-embedded, and sectioned at 4 μm. TUNEL staining was performed according to the manufacturer's instructions (Beyotime, C1098). After deparaffinization and rehydration, sections were treated for antigen exposure and incubated with TUNEL reaction mixture. Apoptotic cells were identified based on positive signals under microscopy.

Immunohistochemistry (IHC)

Paraffin sections were permeabilized with 0.5% Triton X-100 (20 min) and washed with PBS. Endogenous peroxidase activity was quenched using 3% H_2O_2 (15 min). Sections were incubated with primary antibodies (1:50); PBS served as the negative control. After PBS washes, HRP-conjugated secondary antibodies (1:50) were applied for 1 h. DAB was used for chromogenic detection, followed by hematoxylin counterstaining and bluing. Sections were dehydrated through graded ethanol, cleared in xylene, and mounted with resin medium.

Statistical analysis

Data were analyzed using SPSS 23 and are presented as mean ± SD. Normality and homogeneity of variance were assessed prior to parametric testing. For normally distributed data with equal variances, comparisons among groups were performed using one-way ANOVA with appropriate post hoc tests. Otherwise, the Kruskal-Wallis test was applied. A two-tailed $P < 0.05$ was considered statistically significant.

Results

Banxia Xiexin Decoction containing-serum promotes apoptosis in gastric cancer cells

CCK-8 analysis demonstrated a dose-dependent reduction in gastric cancer cell viability following treatment with BXD-containing serum, with the strongest effect observed at 20%, which was selected for subsequent experiments (**Figure 1A**).

Flow cytometry showed that BXD-containing serum significantly increased apoptosis compared with blank rat serum ($P < 0.001$; **Figure 1B**, **1C**). Immunofluorescence staining revealed a marked decrease in stress granule (SG) formation after BXD treatment ($P < 0.001$; **Figure 1D**, **1E**). Consistently, Western blot analysis indicated reduced expression of multidrug resistance-related proteins, including MDR ($P < 0.001$), MRP ($P < 0.01$), and LRP ($P < 0.001$) (**Figure 1F-I**).

hBMSC-derived exosomes enhance chemoresistance in gastric cancer cells

Cultured hBMSCs exhibited the typical spindle-shaped morphology under light microscopy (**Figure 2A**). Transmission electron microscopy confirmed that isolated vesicles displayed characteristic cup-shaped morphology (**Figure 2B**). Western blotting verified the presence of exosomal markers CD9 and SDCBP (**Figure 2C**).

Treatment with 20 μg/mL hBMSC-derived exosomes significantly increased cell viability (**Figure 2D**). Notably, exosome treatment most effectively enhanced resistance in cells exposed to 1 μg/mL oxaliplatin (**Figure 2E**), indicating a strong pro-survival effect under chemotherapeutic stress.

BXD-containing serum suppresses exosome-mediated chemoresistance via the G3BP1-YWHAZ axis in vitro

Oxaliplatin (5 μg/mL) significantly reduced cell viability ($P < 0.001$), whereas hBMSC-derived exosomes (20 μg/mL) partially restored cell survival ($P < 0.01$). Importantly, BXD-containing serum reversed this exosome-induced survival advantage and further reduced viability ($P < 0.001$, **Figure 3A**). Flow cytometric analysis demonstrated that oxaliplatin induced apoptosis, which was attenuated by hBMSC-derived exosomes ($P < 0.001$). BXD-containing serum restored apoptotic levels despite the exosome treatment ($P < 0.001$; **Figure 3B**, **3C**). Western blot (WB) analysis revealed that hBMSC-Exo markedly upregulated the expression of chemoresistance-associated proteins MDR, MRP, and LRP (all $P < 0.001$). In contrast, Banxia Xiexin Decoction-containing serum counteracted this effect, markedly suppressing the levels of all three proteins ($P < 0.001$ for each) (**Figure 3D-G**). Immunofluorescence analysis showed prominent co-localization of G3BP1 and YWHAZ in control

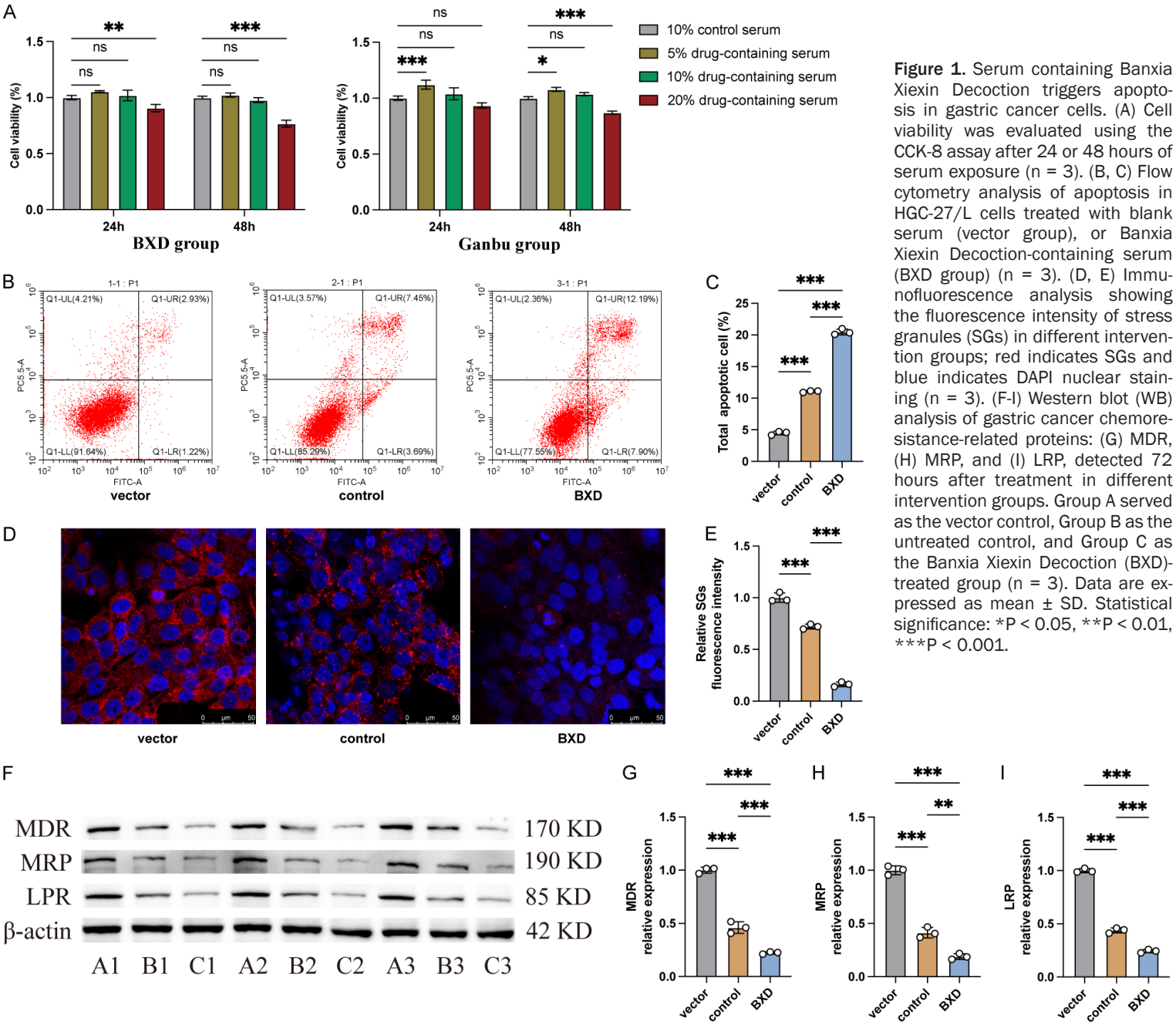

Figure 1. Serum containing Banxia Xiexin Decoction triggers apoptosis in gastric cancer cells. (A) Cell viability was evaluated using the CCK-8 assay after 24 or 48 hours of serum exposure (n = 3). (B, C) Flow cytometry analysis of apoptosis in HGC-27/L cells treated with blank serum (vector group), or Banxia Xiexin Decoction-containing serum (BXD group) (n = 3). (D, E) Immunofluorescence analysis showing the fluorescence intensity of stress granules (SGs) in different intervention groups; red indicates SGs and blue indicates DAPI nuclear staining (n = 3). (F-I) Western blot (WB) analysis of gastric cancer chemoresistance-related proteins: (G) MDR, (H) MRP, and (I) LRP, detected 72 hours after treatment in different intervention groups. Group A served as the vector control, Group B as the untreated control, and Group C as the Banxia Xiexin Decoction (BXD)-treated group (n = 3). Data are expressed as mean ± SD. Statistical significance: *P < 0.05, **P < 0.01, ***P < 0.001.

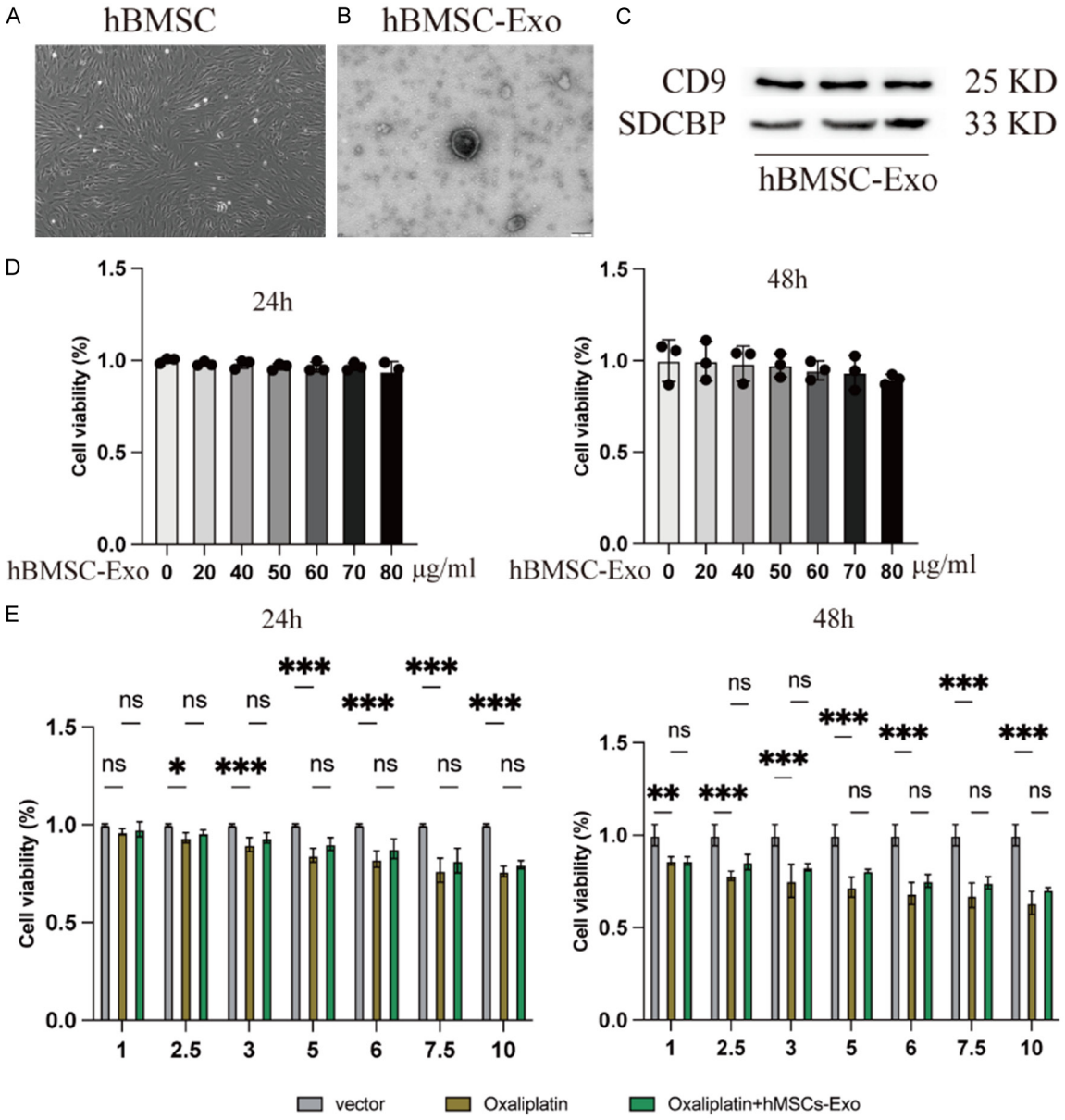

Figure 2. hBMSC-derived exosomes enhance chemoresistance of gastric cancer cells. A. Morphology of hBMSCs observed under a light microscope. B. Morphology of hBMSC-derived exosomes visualized by transmission electron microscopy (TEM). C. The presence of exosomal markers CD9 and SDCBP in the vesicles was confirmed by Western blot (WB) analysis. D. CCK-8 assay showing the proliferation of drug-resistant gastric cancer cells treated with different concentrations of exosomes for 24 or 48 hours (n = 3). E. CCK-8 assay measuring changes in chemoresistance of gastric cancer drug-resistant cell lines 24 or 48 hours after exosome treatment (n = 3). Data are displayed as mean ± SD. *P < 0.05, **P < 0.01, ***P < 0.001.

cells. Oxaliplatin reduced this interaction, whereas exosome treatment restored co-localization. BXD-containing serum markedly disrupted G3BP1-YWHAZ co-localization (**Figure 3H**). Co-immunoprecipitation further confirmed a direct interaction between G3BP1 and YWHAZ (**Figure 3I**).

BXD-containing serum reverses exosome-induced chemoresistance in vivo

A subcutaneous xenograft model was successfully established. During oxaliplatin treatment, hBMSC-derived exosomes significantly accelerated tumor growth (P < 0.001). In contrast,

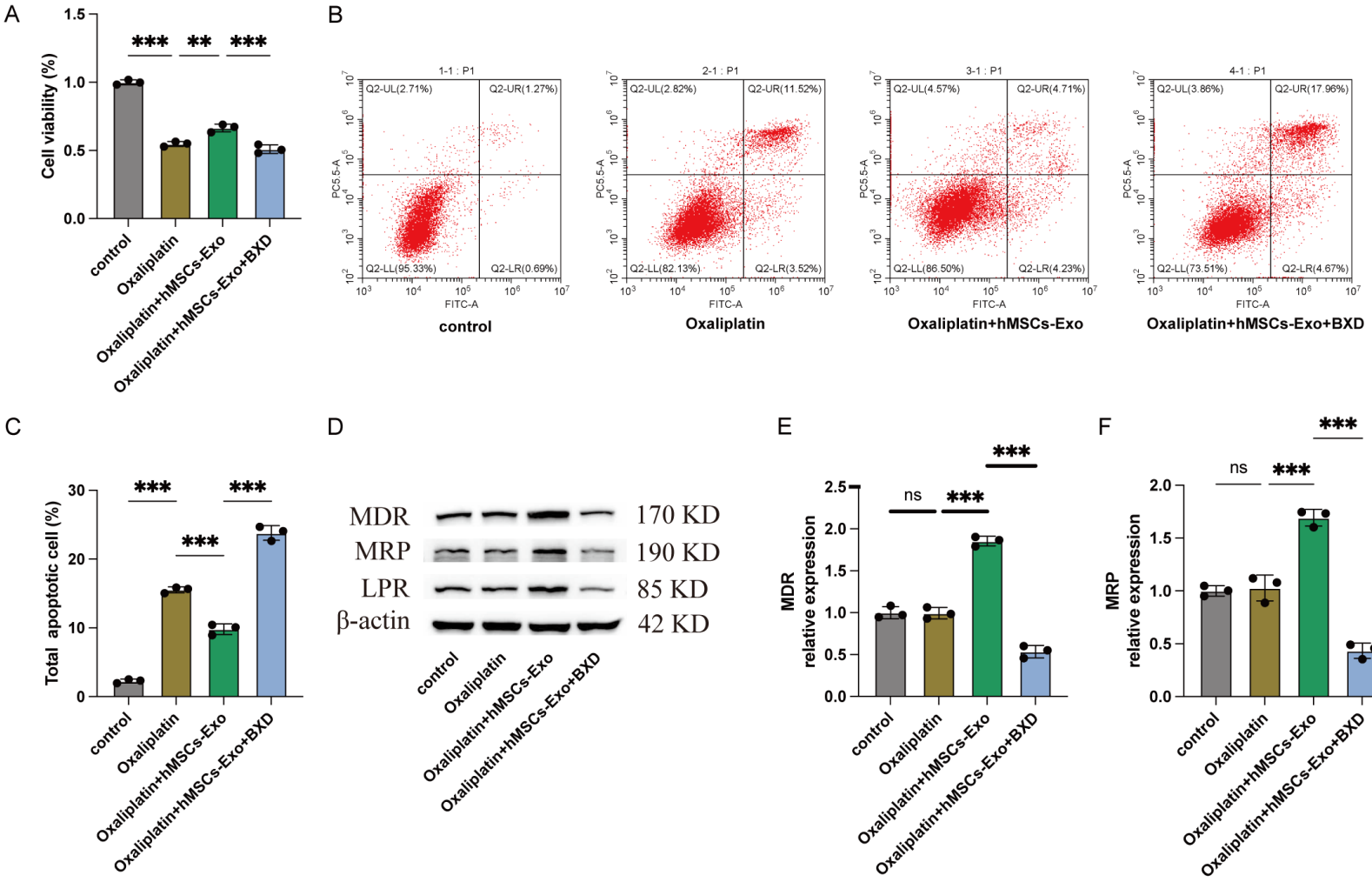
A
Cell viability (%)
control
Oxaliplatin
Oxaliplatin+hMSCs-Exo
Oxaliplatin+hMSCs-Exo+BXD
B
1-1 : P1
Q2-UL(2.71%)
Q2-UR(1.27%)
Q2-LL(95.33%)
Q2-LR(0.69%)
control
2-1 : P1
Q2-UL(2.82%)
Q2-UR(11.52%)
Q2-LL(82.13%)
Q2-LR(3.52%)
Oxaliplatin
3-1 : P1
Q2-UL(4.57%)
Q2-UR(4.71%)
Q2-LL(86.50%)
Q2-LR(4.23%)
Oxaliplatin+hMSCs-Exo
4-1 : P1
Q2-UL(3.86%)
Q2-UR(17.96%)
Q2-LL(73.51%)
Q2-LR(4.67%)
Oxaliplatin+hMSCs-Exo+BXD
PC5.5-A
FITC-A
C
Total apoptotic cell (%)
D
MDR
MRP
LPR
β-actin
170 KD
190 KD
85 KD
42 KD
E
MDR relative expression
ns
F
MRP relative expression

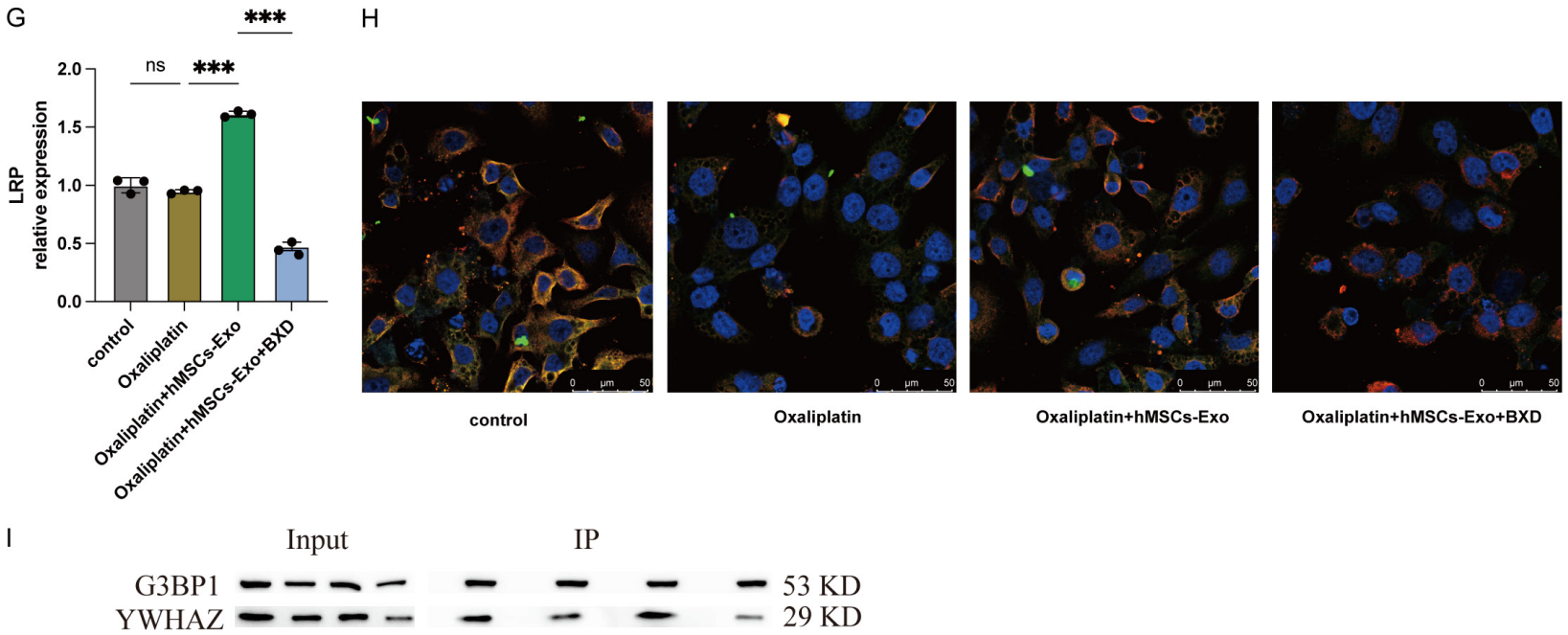

Figure 3. By targeting the G3BP1/YWHAZ axis, Banxia Xiexin Decoction-containing serum suppresses hBMSC-Exo-induced chemoresistance in gastric cancer cells. (A) CCK-8 assay assessing the proliferation capacity of gastric cancer cells under different intervention conditions (n = 3); (B, C) Apoptosis in HGC-27/L cells was assessed by flow cytometry across three independent experiments (n = 3) in distinct intervention groups; (D-G) Western blot (WB) analysis of gastric cancer chemoresistance-related proteins: (E) MDR, (F) MRP, and (G) LRP, in different intervention groups (n = 3); (H) Immunofluorescence analysis showing the co-localization of G3BP1 and YWHAZ; red fluorescence indicates G3BP1; green fluorescence indicates YWHAZ; and blue fluorescence indicates DAPI-stained nuclei. Apoptosis in HGC-27/L cells was assessed by flow cytometry across three independent experiments (n = 3) in distinct intervention groups. (I) Co-immunoprecipitation (Co-IP) verifies the physical association between G3BP1 and YWHAZ. Data are shown as mean ± SD. *P < 0.05, **P < 0.01, ***P < 0.001.

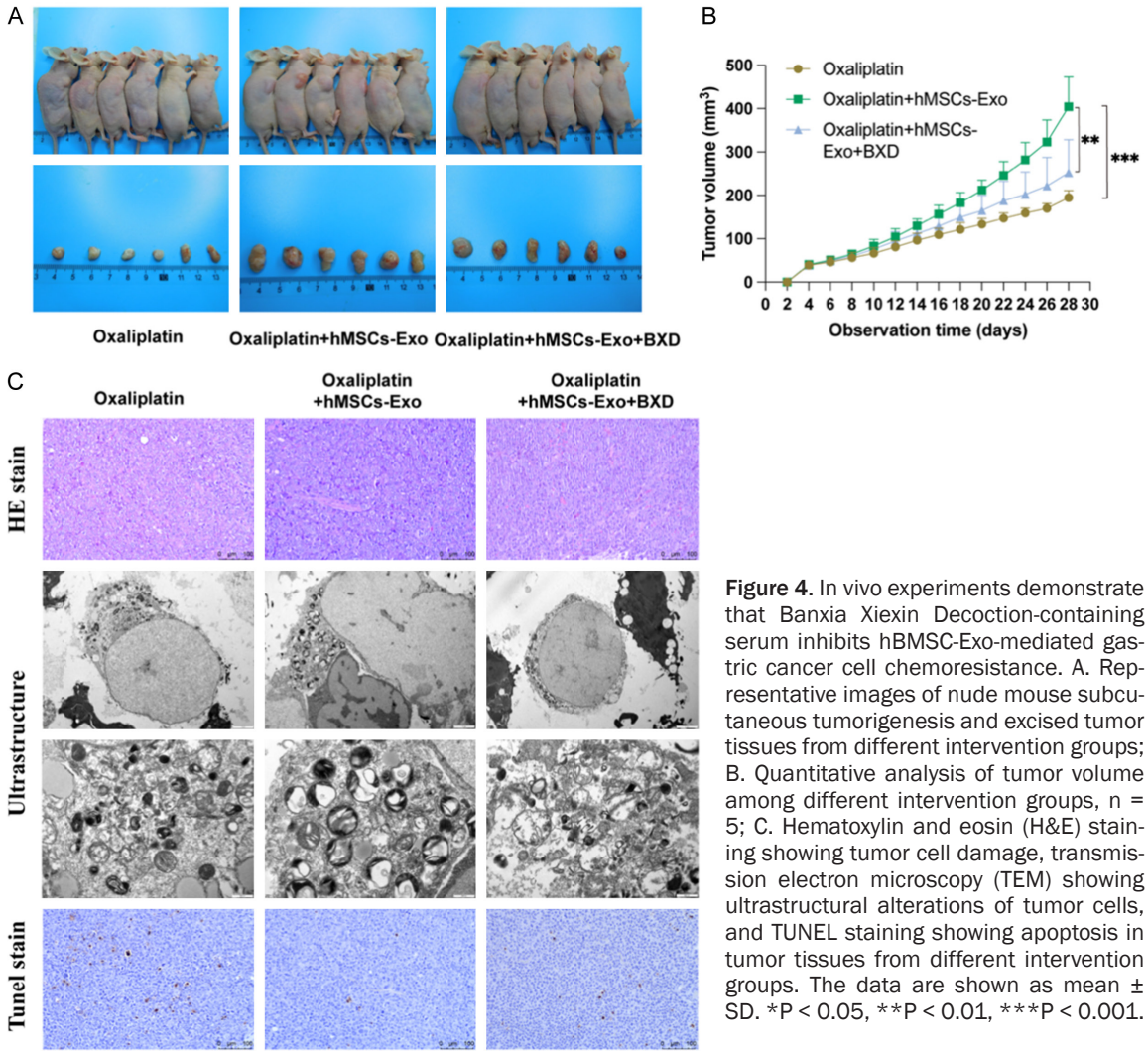

Figure 4. In vivo experiments demonstrate that Banxia Xiexin Decoction-containing serum inhibits hBMSC-Exo-mediated gastric cancer cell chemoresistance. A. Representative images of nude mouse subcutaneous tumorigenesis and excised tumor tissues from different intervention groups; B. Quantitative analysis of tumor volume among different intervention groups, n = 5; C. Hematoxylin and eosin (H&E) staining showing tumor cell damage, transmission electron microscopy (TEM) showing ultrastructural alterations of tumor cells, and TUNEL staining showing apoptosis in tumor tissues from different intervention groups. The data are shown as mean ± SD. *P < 0.05, **P < 0.01, ***P < 0.001.

BXD-containing serum attenuated this effect and significantly inhibited tumor progression (P < 0.01, **Figure 4A**, **4B**). Histological analysis (H&E) revealed that exosomes reduced oxaliplatin-induced tumor cell damage, whereas BXD restored tumor cell injury (**Figure 4C**). Transmission electron microscopy demonstrated that exosomes alleviated ultrastructural damage induced by oxaliplatin, while BXD treatment promoted structural disruption. TUNEL staining showed that exosomes suppressed apoptosis in tumor tissues, and BXD reversed this effect, increasing apoptotic cell numbers (**Figure 4C**).

BXD modulates the G3BP1-YWHAZ pathway in vivo

Immunohistochemistry demonstrated that hBMSC-derived exosomes increased expression of MDR, MRP, LRP, Ki67, and SG-related proteins following the oxaliplatin treatment. These elevations were significantly reduced by BXD-containing serum (**Figure 5A**). Immunofluorescence staining confirmed that exosomes restored G3BP1-YWHAZ co-localization suppressed by oxaliplatin, whereas BXD disrupted this interaction (**Figure 5B**). Western blot analysis showed that exosome treatment reduced pro-apoptotic proteins (Bax, cleaved PARP, cleaved caspase-9, and cleaved caspase-3) (P < 0.001). BXD-containing serum reversed this suppression and significantly increased apoptotic marker expression (P < 0.01; **Figure 5C-G**).

Discussion

Exosomes are internalized by recipient cells primarily through endocytic pathways and serve as essential mediators of intercellular commu-

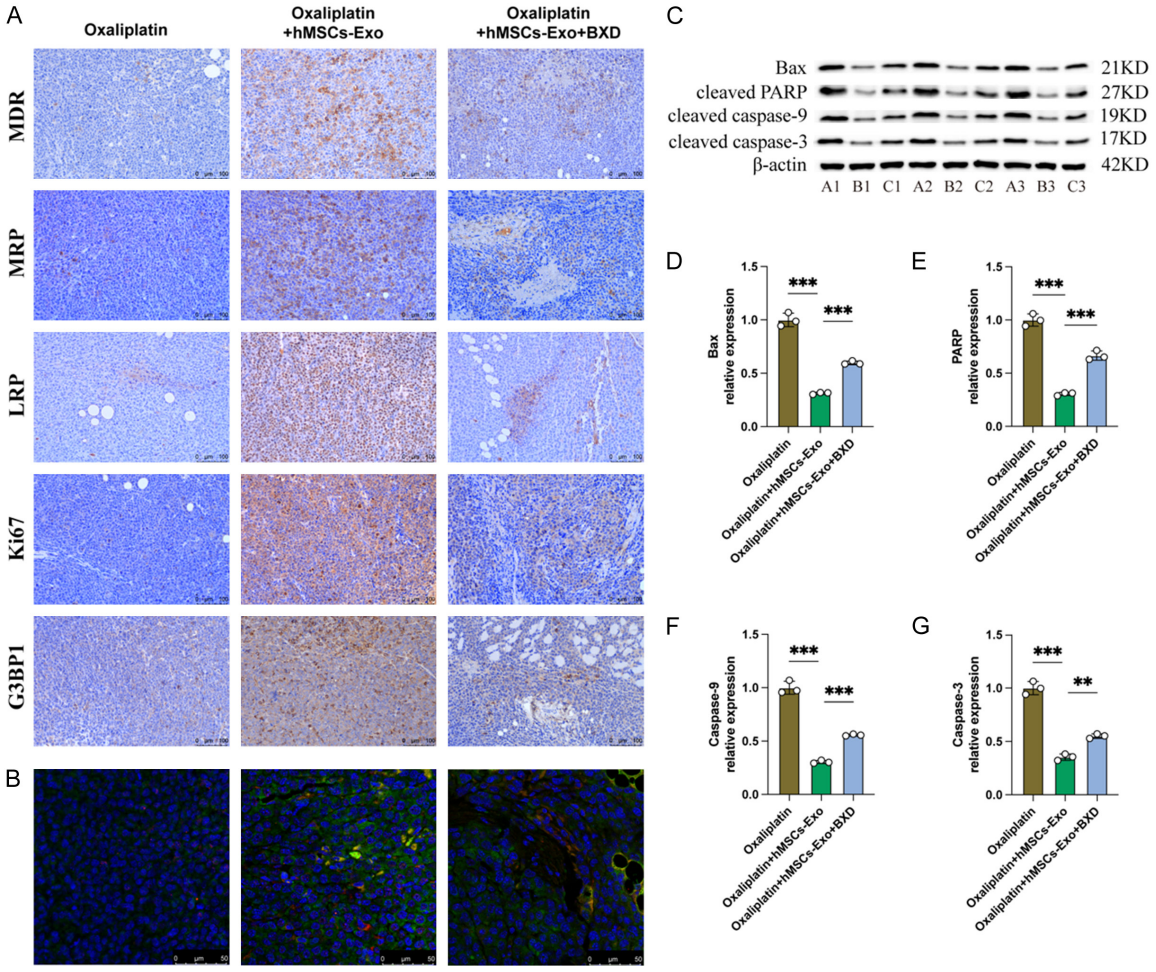

Figure 5. In vivo experiments demonstrate that Banxia Xiexin Decoction-containing serum inhibits hBMSC-Exo-mediated gastric cancer cell chemoresistance by targeting the G3BP1/YWHAZ axis. A. Immunohistochemical (IHC) analysis showing the levels of expression for MDR, MRP, LRP, Ki67, and G3BP1 in tumor tissues from different intervention groups; B. Immunofluorescence analysis showing the co-localization of G3BP1 and YWHAZ in tumor tissues from different intervention groups; C-G. Analysis of apoptotic markers in tumor tissues from different intervention groups using Western blot (WB), focusing on Bax, cleaved PARP, cleaved caspase-9, and cleaved caspase-3. Results are presented as mean ± SD. *P < 0.05, **P < 0.01, ***P < 0.001.

nication within the tumor microenvironment [31, 32]. Accumulating evidence indicates that exosomes contribute to the acquisition of chemoresistance in multiple malignancies. In gastric cancer, MSC-derived exosomes have been reported to enhance resistance both in vitro and in vivo [10, 11]. Consistent with previous studies [16, 17, 33], our findings further demonstrate that MSC-derived exosomes significantly reduce oxaliplatin sensitivity in gastric cancer cells, promoting survival and attenuating apoptosis. These results reinforce the concept that stromal-tumor interactions mediated by exosomes are critical determinants of therapeutic response.

Stress granules (SGs) represent a conserved adaptive response to cellular stress, including chemotherapy. Under cytotoxic conditions, untranslated mRNAs and associated proteins aggregate to form SGs, thereby facilitating cellular survival [34-36]. G3BP1 is a central scaffolding protein required for SG assembly and functional maintenance. Previous reports have shown that G3BP1 interacts with YWHA family proteins, including YWHAZ, to suppress Bax expression and enhance anti-apoptotic signaling in gastric cancer [22, 37]. In the present study, we observed that MSC-derived exosomes promoted G3BP1-YWHAZ co-localization and strengthened their interaction, accom-

panied by reduced apoptotic signaling. These findings support the notion that the G3BP1-YWHAZ axis functions as a pivotal molecular bridge linking stress granule dynamics to chemoresistance [22].

Importantly, Banxia Xiexin Decoction effectively counteracted these effects. BXD-containing serum induced apoptosis, reduced SG formation, and downregulated MDR-related proteins in vitro. Mechanistically, BXD disrupted the interaction between G3BP1 and YWHAZ, thereby restoring Bax expression and caspase activation. In xenograft models, BXD reversed exosome-mediated resistance, increased pro-apoptotic markers, and suppressed tumor growth during oxaliplatin treatment. Together, these results suggest that BXD enhances chemosensitivity by targeting an exosome-driven anti-apoptotic signaling cascade rather than acting solely as a direct cytotoxic agent.

Several limitations merit consideration. First, the specific cargo within MSC-derived exosomes responsible for modulating the G3BP1-YWHAZ interaction was not identified. Comprehensive exosomal profiling and functional validation will be necessary to clarify this upstream regulatory mechanism. Second, although BXD disrupted the G3BP1-YWHAZ axis, it remains unclear whether the decoction directly influences exosome production, cargo composition, or uptake, and the drug-containing serum contains a complex mixture of unknown bioactive compounds and metabolites, whose concentrations are difficult to control or quantify. Therefore, it remains unclear whether the observed effects are due to specific active ingredients, synergistic interactions with serum components, or indirect consequences of systemic metabolism. Third, rescue experiments were not performed to definitively establish causality between the G3BP1-YWHAZ interaction and apoptotic regulation. Fourth, the mechanistic findings were derived from a single gastric cancer cell line and require confirmation in additional models. Finally, the use of rat-derived drug-containing serum introduces variability in active compound composition and limits precise pharmacokinetic interpretation. Future studies integrating chemical characterization, targeted molecular approaches, and multi-model validation will be essential to further define the active constituents and their mechanisms.

Overall, this study identifies that Banxia Xiexin Decoction modulates exosome-mediated signaling pathways involving the G3BP1-YWHAZ axis and provides experimental evidence that it can modulate this axis to restore chemosensitivity.

Acknowledgements

This study was supported by the National Natural Science Foundation of China (No. 82260895).

Disclosure of conflict of interest

None.

Address correspondence to: Xiping Liu, Gansu University of Chinese Medicine, No. 35, Ding Xi East Road, Cheng Guan District, Lanzhou 730000, Gansu, China. E-mail: lxpd-257@163.com; Kun Niu, College of Traditional Chinese Medicine, Hainan Medical University, Haikou 571199, Hainan, China. E-mail: kunniuniu@163.com

References

[1] Han B, Zheng R, Zeng H, Wang S, Sun K, Chen R, Li L, Wei W and He J. Cancer incidence and mortality in China, 2022. J Natl Cancer Cent 2024; 4: 47-53.

[2] Duan Y, Xu Y, Dou Y and Xu D. Helicobacter pylori and gastric cancer: mechanisms and new perspectives. J Hematol Oncol 2025; 18: 10.

[3] Liu J, Yuan Q, Guo H, Guan H, Hong Z and Shang D. Deciphering drug resistance in gastric cancer: potential mechanisms and future perspectives. Biomed Pharmacother 2024; 173: 116310.

[4] Zhang SX, Liu W, Ai B, Sun LL, Chen ZS and Lin LZ. Current advances and outlook in gastric cancer chemoresistance: a review. Recent Pat Anticancer Drug Discov 2022; 17: 26-41.

[5] Yasuda T and Wang YA. Gastric cancer immunosuppressive microenvironment heterogeneity: implications for therapy development. Trends Cancer 2024; 10: 627-642.

[6] Ramírez Idarraga JA and Restrepo Múnera LM. Mesenchymal stem cells: their role in the tumor microenvironment. Tissue Eng Part B Rev 2023; 29: 681-691.

[7] Uccelli A, Moretta L and Pistoia V. Mesenchymal stem cells in health and disease. Nat Rev Immunol 2008; 8: 726-736.

[8] Zhang Y, Wang C and Li JJ. Revisiting the role of mesenchymal stromal cells in cancer initiation, metastasis and immunosuppression. Exp Hematol Oncol 2024; 13: 64.

[9] Guo S, Huang C, Han F, Chen B, Ding Y, Zhao Y, Chen Z, Wen S, Wang M, Shen B and Zhu W. Gastric cancer mesenchymal stem cells inhibit NK cell function through mTOR signalling to promote tumour growth. Stem Cells Int 2021; 2021: 9989790.
[10] Shen J, Huang C, Cui L, Zhao Y, Zhu M, Chen Z, Wang M, Zhu W and Shen B. Chemotherapeutic drugs endow gastric cancer mesenchymal stem cells with stronger tumor-promoting ability. J Environ Pathol Toxicol Oncol 2024; 43: 1-13.
[11] Ramuta T and Kreft ME. Mesenchymal stem/stromal cells may decrease success of cancer treatment by inducing resistance to chemotherapy in cancer cells. Cancers (Basel) 2022; 14: 3761.
[12] Ullah M, Akbar A, Ng NN, Concepcion W and Thakor AS. Mesenchymal stem cells confer chemoresistance in breast cancer via a CD9 dependent mechanism. Oncotarget 2019; 10: 3435-3450.
[13] Lyu T, Wang Y, Li D, Yang H, Qin B, Zhang W, Li Z, Cheng C, Zhang B, Guo R and Song Y. Exosomes from BM-MSCs promote acute myeloid leukemia cell proliferation, invasion and chemoresistance via upregulation of S100A4. Exp Hematol Oncol 2021; 10: 24.
[14] Huang F, Cao X, Mei J, Wu C, Zhu W, Sun L, Dai C and Wang M. Gastric cancer cells shuttle lactate to induce inflammatory CAF-like phenotype and function in bone marrow-derived mesenchymal stem cells. Mol Immunol 2025; 183: 93-103.
[15] Wu H, Fu M, Liu J, Chong W, Fang Z, Du F, Liu Y, Shang L and Li L. The role and application of small extracellular vesicles in gastric cancer. Mol Cancer 2021; 20: 71.
[16] Ji R, Zhang B, Zhang X, Xue J, Yuan X, Yan Y, Wang M, Zhu W, Qian H and Xu W. Exosomes derived from human mesenchymal stem cells confer drug resistance in gastric cancer. Cell Cycle 2015; 14: 2473-2483.
[17] Easwaran VB, Pai KMS and Pai KSR. Mesenchymal stem cell-derived exosomes in cancer resistance against therapeutics. Cancers (Basel) 2025; 17: 831.
[18] Tai CJ, Hsu CH, Shen SC, Lee WR and Jiang MC. Cellular apoptosis susceptibility (CSE1L/CAS) protein in cancer metastasis and chemotherapeutic drug-induced apoptosis. J Exp Clin Cancer Res 2010; 29: 110.
[19] Blagosklonny MV. Cell death beyond apoptosis. Leukemia 2000; 14: 1502-1508.
[20] Moyer A, Tanaka K and Cheng EH. Apoptosis in cancer biology and therapy. Annu Rev Pathol 2025; 20: 303-328.
[21] Ma S, Zhou M, Xu Y, Gu X, Zou M, Abudushalamu G, Yao Y, Fan X and Wu G. Clinical application and detection techniques of liquid biopsy in gastric cancer. Mol Cancer 2023; 22: 7.
[22] Zhao J, Fu X, Chen H, Min L, Sun J, Yin J, Guo J, Li H, Tang Z, Ruan Y, Wang X, Sun Y and Huang L. G3BP1 interacts with YWHAZ to regulate chemoresistance and predict adjuvant chemotherapy benefit in gastric cancer. Br J Cancer 2021; 124: 425-436.
[23] Chen RX, Mo AT, Xu SD, Wu JH, Deng MH, Xie SH, Zhuang WT, Duan JL, Yang H, Lin P, He Z, Tang JM, Zhou HY, Ben XS, Qiao GB and Xie D. m6A-mediated circG3BP1 translocation to stress granules promotes nucleation and senescence-linked chemoresistance. Cell Rep 2025; 44: 116375.
[24] Lin J, Wang J, Zhao K, Li Y, Zhang X and Sheng J. Molecular targets and mechanisms of traditional Chinese medicine combined with chemotherapy for gastric cancer: a meta-analysis and multi-omics approach. Ann Med 2025; 57: 2494671.
[25] Ling CQ. Cancerous toxin is the key pathogenic factor of malignant tumor. Zhong Xi Yi Jie He Xue Bao 2008; 6: 111-114.
[26] Dai Z, Tan C, Wang J, Wang Q, Wang Y, He Y, Peng Y, Gao M, Zhang Y, Liu L, Song N and Li N. Traditional Chinese medicine for gastric cancer: an evidence mapping. Phytother Res 2024; 38: 2707-2723.
[27] Feng X, Xue F, He G, Ni Q and Huang S. Banxia xiexin decoction affects drug sensitivity in gastric cancer cells by regulating MGMT expression via IL-6/JAK/STAT3-mediated PD-L1 activity. Int J Mol Med 2021; 48: 165.
[28] Li Y, Li L, Wang X, Huang H and Han T. Determining the mechanism of Banxia Xiexin Decoction for gastric cancer treatment through network analysis and experimental validation. ACS Omega 2024; 9: 10119-10131.
[29] Deng C, Huo M, Chu H, Zhuang X, Deng G, Li W, Wei H, Zeng L, He Y, Liu H, Li J, Zhang C and Chen H. Exosome circATP8A1 induces macrophage M2 polarization by regulating the miR-1-3p/STAT6 axis to promote gastric cancer progression. Mol Cancer 2024; 23: 49.
[30] Xu J, Fang S, Dong X, Liang C, Yang R, Zhao Y, Gu H, Fu M, Zhang J, Zhang X, Zhang X and Ji R. Hypoxia-induced upregulation of HIF1A-AS3 promotes MSC transition to cancer-associated fibroblasts and confers drug resistance in gastric cancer. Drug Resist Updat 2025; 82: 101275.
[31] Liang Y, Duan L, Lu J and Xia J. Engineering exosomes for targeted drug delivery. Theranostics 2021; 11: 3183-3195.
[32] Kalluri R and LeBleu VS. The biology, function, and biomedical applications of exosomes. Science 2020; 367: eaau6977.

[33] Lin Z, Wu Y, Xu Y, Li G, Li Z and Liu T. Mesenchymal stem cell-derived exosomes in cancer therapy resistance: recent advances and therapeutic potential. Mol Cancer 2022; 21: 179.
[34] Fujikawa D, Nakamura T, Yoshioka D, Li Z, Moriizumi H, Taguchi M, Tokai-Nishizumi N, Kozuka-Hata H, Oyama M and Takekawa M. Stress granule formation inhibits stress-induced apoptosis by selectively sequestering executioner caspases. Curr Biol 2023; 33: 1967-1981, e1968.
[35] Shi X, Si X, Zhang E, Zang R, Yang N, Cheng H, Zhang Z, Pan B and Sun Y. Paclitaxel-induced stress granules increase LINE-1 mRNA stability to promote drug resistance in breast cancer cells. J Biomed Res 2021; 35: 411-424.
[36] Gao X, Jiang L, Gong Y, Chen X, Ying M, Zhu H, He Q, Yang B and Cao J. Stress granule: a promising target for cancer treatment. Br J Pharmacol 2019; 176: 4421-4433.
[37] Malvi P, Reddy DS, Kumar R, Chava S, Burela S, Parajuli K, Zhang X and Wajapeyee N. LIMK2 promotes melanoma tumor growth and metastasis through G3BP1-ESM1 pathway-mediated apoptosis inhibition. Oncogene 2023; 42: 1478-1491.